

Unveiling the structure of pseudoscalar mesons

Khépani Raya* and Lei Chang

School of Physics, Nankai University, Tianjin 300071, China

**E-mail: khepani@nankai.edu.cn*

Minghui Ding and Daniele Binosi

*European Centre for Theoretical Studies in Nuclear Physics and Related Areas
(ECT*) and Fondazione Bruno Kessler*

Villa Tambosi, Strada delle Tabarelle 286, I-38123 Villazzano (TN) Italy

Craig D. Roberts

*School of Physics, Nanjing University, Nanjing, Jiangsu 210093, China
Institute for Nonperturbative Physics, Nanjing University, Nanjing, Jiangsu 210093,
China*

A valuable approach to the analysis of hadron physics observables is provided by QCD's equations-of-motion; namely, the Dyson-Schwinger equations. Drawing from a diverse collection of predictions, we revisit: $\gamma\gamma^* \rightarrow$ neutral pseudoscalar transition form factors, their corresponding valence-quark distribution amplitudes and a recent result on the pion distribution functions.

Keywords: Dyson-Schwinger equations, distribution amplitudes, distribution functions, transition form factors.

1. Introduction

In an exciting era of ongoing and forthcoming experiments, the Dyson-Schwinger equation (DSE) approach to QCD, which describes hadrons in terms of quarks and gluons, is placed as a promising tool for hadron physics¹⁻³. The present manuscript sums up a collection of DSE results on the pseudoscalar mesons: valence-quark distribution amplitudes (PDAs)⁴⁻⁶, $\gamma^*\gamma^* \rightarrow M$ transition form factors (TFFs)⁶⁻⁹ and the pion distribution functions (PDF)¹⁰.

2. Valence-quark distribution amplitudes

Given a pseudoscalar meson M with mass m_M , the PDA, $\phi_M(x; \zeta)$, is defined as the projection onto the light-front of its Bethe-Salpeter wave-

2

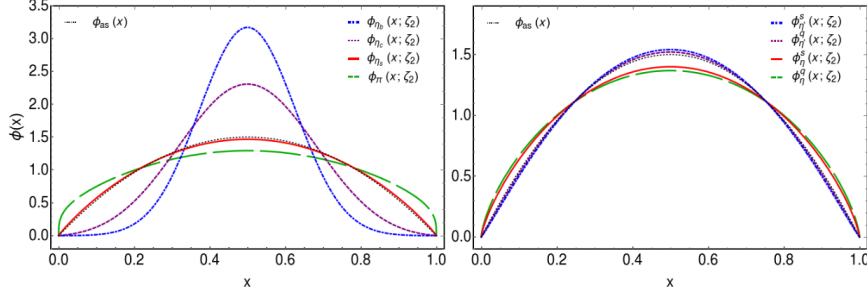


Fig. 1. PDAs at ζ_2 and the asymptotic profile¹¹, $\phi_{\text{as}}(x) := 6x(1-x)$. The η_s corresponds to a pseudoscalar with s -massive valence-quarks. Due to the dominance of dynamical chiral symmetry breaking (DCSB), $\phi_\pi(x; \zeta_2)$ is broader than $\phi_{\text{as}}(x)$, while those corresponding to $\eta_{c,b}$, more influenced by the Higgs mechanism, are narrower. Lying close to $\phi_{\text{as}}(x)$, we find the η_s , η and η' PDAs. There is an interplay between strong and weak mass generation being dominant and the s -quark is the boundary^{5,6}.

function, $\chi_M(q; P) = S(q^+) \Gamma_M(q; P) S(q^-)$, such that:

$$\phi_M(x; \zeta) = \frac{Z_2}{f_M} \text{tr}_{\text{CD}} \int_q \delta_n^x(q^+) \gamma_5 \gamma \cdot n \chi_M(q; P), \quad \int_0^1 dx \phi_M(x; \zeta) = 1, \quad (1)$$

$$\delta_n^x(q^+) = \delta(n \cdot q^+ - x n \cdot P), \quad q^+ = q + \eta P, \quad q^- = q - (1 - \eta)P,$$

where $\int_q := \int \frac{d^4 q}{(2\pi)^4}$, $\eta \in [0, 1]$ defines the relative momentum between the quark/antiquark, f_M is the corresponding decay constant, Z_2 is the quark wavefunction renormalization constant and n is a light-like four vector ($n^2 = 0$, $n \cdot P = -m_M$). Computation of several Mellin moments allow to reconstruct the PDA⁴⁻⁶. A selection of PDAs is shown in Fig. 1.

3. $\gamma^* \gamma^* \rightarrow M$ transition form factors

In the impulse approximation (IA), the transition $\gamma^* \gamma^* \rightarrow M$ reads as⁹:

$$T_{\mu\nu}(Q_1, Q_2) = \frac{e^2}{4\pi^2} \epsilon_{\mu\nu\alpha\beta} Q_{1\alpha} Q_{2\beta} G_M(Q_1^2, Q_1 \cdot Q_2, Q_2^2) \quad (2)$$

$$= \mathbf{e}_f^2 \text{tr}_{\text{CD}} \int_q i\chi_\mu^f(q, q_1) \Gamma_M(q_1, q_2) S_f(q_2) i\Gamma_\nu^f(q_2, q),$$

where Q_1 , Q_2 are the momenta of the two photons. The kinematic arrangement is $q_1 = q + Q_1$, $q_2 = q - Q_2$; \mathbf{e}_f^2 is a charge factor associated with the meson's valence quarks. Γ_M is the pseudoscalar Bethe-Salpeter amplitude (BSA). The amputated (Γ_ν) and non amputated (χ_μ) quark-photon vertices can be properly expressed via the quark propagator dressing functions⁷. BSAs and quark propagators are obtained (at $\zeta = \zeta_2$) in the

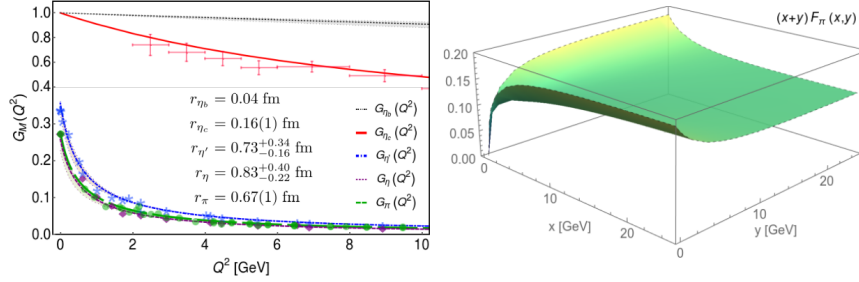


Fig. 2. **Left panel.** DSE predictions of $\gamma\gamma^* \rightarrow M$ TFFs and a variety of experimental data (CELLO, CLEO, Babar, Belle, L3 and PDG) for η_c (error bars), η' (asterisks), η (diamonds) and π^0 (circles). See Ref. 9 for a complete list of data sources. The $\eta_{c,b}$ results are normalized to $G_M(0) = 1$ and the band surrounding the η_b corresponds to the non-relativistic QCD result of Ref. 13. Those form factors can be found, on a larger domain, in Refs. 6–8. **Right panel.** $\gamma^*\gamma^* \rightarrow \pi^0$ TFF⁹. The ultraviolet limit constraints¹¹ are preserved while simultaneously reproducing the empirical value at $Q^2 \rightarrow 0$.

rainbow-ladder approximation, self-consistent with the IA^a. Via perturbation theory integral representations of those objects, the complete results basically require a series of perturbation-theory-like integrals. A similar approach was followed for the pion electromagnetic form factor¹². The computed TFFs are displayed in Figs. 2.

4. Pion distribution functions

Detailed considerations have yielded the following symmetry-preserving expression^{10,14} for the pion valence-quark PDF, $q_V(x; \zeta)$:

$$q_V(x; \zeta) = \text{tr}_{\text{CD}} \int_q \delta_n^x(q^+) n \cdot \partial_{q^+} [\Gamma_{\pi}(q^+; -P) S(q^+)] \Gamma_{\pi}(q^-; P) S(q^-). \quad (3)$$

The renormalization scale ($\zeta = \zeta_H \sim 0.3$ GeV) is defined such that the fully dressed (valence-quarks) quasiparticles are the correct degrees of freedom¹⁵, $\int_0^1 dx q_V(x; \zeta_H) = 1$. We reconstruct $q_V(x; \zeta_H)$ from its Mellin moments and evolve through DGLAP equations to incorporate gluon and sea content in the manner that QCD prescribes^{10,15}. This process is detailed in Ref. 10 and the obtained PDFs are shown in Fig. 3.

^aThe non-Abelian anomaly is introduced in the Bethe-Salpeter kernel of the $\eta - \eta'$ BSE⁶ and a mild amendment of Eq. (2) is required.

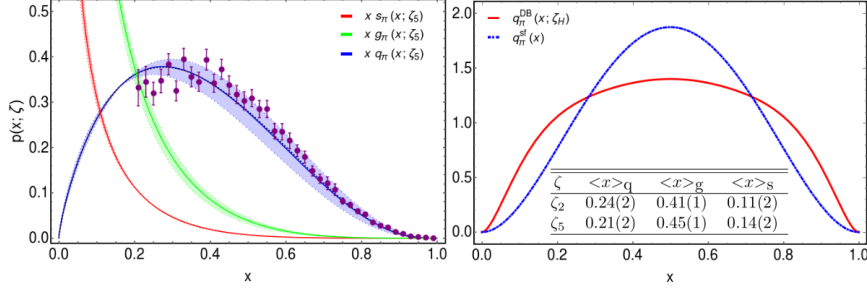


Fig. 3. **Left panel:** valence quark (q_π), gluon (g_π) and sea (s_π) pion PDFs at the experimental scale^{16,17}, $\zeta = 5.2 \text{ GeV} := \zeta_5$. **Right panel:** valence-quark PDF at ζ_H . Here, $q_\pi^{\text{DB}}(x; \zeta_2)$ is the DSE prediction from Ref. 10 and $q_\pi^{\text{sf}}(x) = 30x^2(1-x)^2$ is a scale-free parton-like model¹⁴, the marked broadening of $q_\pi^{\text{DB}}(x; \zeta_2)$ relative to $q_\pi^{\text{sf}}(x)$ is a consequence of DCSB.

5. Conclusions and scope

We have recapitulated predictions for an array of pseudoscalar mesons properties obtained within a single unifying DSE framework. The examples chosen are illustrative, not exhaustive. Analyses of kaon PDFs and meson GPDs and TMDs are currently underway.

6. Acknowledgements

KR wants to acknowledge the local organizers for their hospitality. Work supported by: Jiangsu Province *Hundred Talents Plan for Professionals*.

References

1. Tanja Horn and Craig D. Roberts. The pion: an enigma within the Standard Model. *J. Phys.*, G43(7):073001, 2016.
2. Gernot Eichmann, Helios Sanchis-Alepuz, Richard Williams, Reinhard Alkofer, and Christian S. Fischer. Baryons as relativistic three-quark bound states. *Prog. Part. Nucl. Phys.*, 91:1–100, 2016.
3. Volker D. Burkert and Craig D. Roberts. Colloquium : Roper resonance: Toward a solution to the fifty year puzzle. *Rev. Mod. Phys.*, 91(1):011003, 2019.
4. Lei Chang, I. C. Cloet, J. J. Cobos-Martinez, C. D. Roberts, S. M. Schmidt, and P. C. Tandy. Imaging dynamical chiral symmetry breaking: pion wave function on the light front. *Phys. Rev. Lett.*, 110(13):132001, 2013.

5. Minghui Ding, Fei Gao, Lei Chang, Yu-Xin Liu, and Craig D. Roberts. Leading-twist parton distribution amplitudes of S-wave heavy-quarkonia. *Phys. Lett.*, B753:330–335, 2016.
6. Minghui Ding, Khépani Raya, Adnan Bashir, Daniele Binosi, Lei Chang, Muyang Chen, and Craig D. Roberts. $\gamma^*\gamma \rightarrow \eta, \eta'$ transition form factors. *Phys. Rev.*, D99(1):014014, 2019.
7. K. Raya, L. Chang, A. Bashir, J. J. Cobos-Martinez, L. X. Gutiérrez-Guerrero, C. D. Roberts, and P. C. Tandy. Structure of the neutral pion and its electromagnetic transition form factor. *Phys. Rev.*, D93(7):074017, 2016.
8. Khépani Raya, Minghui Ding, Adnan Bashir, Lei Chang, and Craig D. Roberts. Partonic structure of neutral pseudoscalars via two photon transition form factors. *Phys. Rev.*, D95(7):074014, 2017.
9. Khépani Raya, Adnan Bashir, and Pablo Roig. Contribution of neutral pseudoscalar mesons to a_μ^{HLbL} within a Schwinger-Dyson equations approach to QCD, arXiv:1910.05960 [hep-ph].
10. Minghui Ding, Khépani Raya, Daniele Binosi, Lei Chang, Craig D. Roberts, and Sebastian M. Schmidt. Symmetry, symmetry breaking, and pion parton distributions, arXiv:1905.05208 [nucl-th]. 2019.
11. G. Peter Lepage and Stanley J. Brodsky. Exclusive Processes in Perturbative Quantum Chromodynamics. *Phys. Rev.*, D22:2157, 1980.
12. L. Chang, I. C. Cloet, C. D. Roberts, S. M. Schmidt, and P. C. Tandy. Pion electromagnetic form factor at spacelike momenta. *Phys. Rev. Lett.*, 111(14):141802, 2013.
13. Feng Feng, Yu Jia, and Wen-Long Sang. Can Nonrelativistic QCD Explain the $\gamma\gamma^* \rightarrow \eta_c$ Transition Form Factor Data? *Phys. Rev. Lett.*, 115(22):222001, 2015.
14. Lei Chang, Cédric Mezrag, Hervé Moutarde, Craig D. Roberts, Jose Rodríguez-Quintero, and Peter C. Tandy. Basic features of the pion valence-quark distribution function. *Phys. Lett.*, B737:23–29, 2014.
15. José Rodríguez-Quintero, Lei Chang, Khépani Raya, and Craig D. Roberts. Process-independent effective coupling and the pion structure function, arXiv:1909.13802 [hep-ph].
16. J. S. Conway et al. Experimental Study of Muon Pairs Produced by 252-GeV Pions on Tungsten. *Phys. Rev.*, D39:92–122, 1989.
17. Matthias Aicher, Andreas Schafer, and Werner Vogelsang. Soft-gluon resummation and the valence parton distribution function of the pion. *Phys. Rev. Lett.*, 105:252003, 2010.